

# AN APPOINTMENT WITH REPRODUCING KERNEL HILBERT SPACE GENERATED BY GENERALIZED GAUSSIAN RBF AS $L^2$ -MEASURE

HIMANSHU SINGH

ABSTRACT. Gaussian Radial Basis Function (RBF) Kernels are the most-often-employed kernels in artificial intelligence and machine learning routines for providing optimally-best results in contrast to their respective counter-parts. However, a little is known about the application of the *Generalized Gaussian Radial Basis Function* on various machine learning algorithms namely, kernel regression, support vector machine (SVM) and pattern-recognition via neural networks. The results that are yielded by Generalized Gaussian RBF in the *kernel* sense outperforms in stark contrast to Gaussian RBF Kernel, Sigmoid Function and ReLU Function.

This manuscript demonstrates the application of the *Generalized Gaussian RBF* in the *kernel* sense on the aforementioned machine learning routines along with the comparisons against the aforementioned functions as well. Furthermore, we present the explicit description for the reproducing kernel Hilbert Space that is generated by the measure of Generalized Gaussian RBF in  $L^2$ -measure theoretic sense. Finally, we provide the future directions in terms of eigen-function decomposition and reduced order modeling application of Generalized Gaussian RBF.

## 1. INTRODUCTION

Artificial Intelligence and machine learning algorithms takes the advantage of various important mathematical functions that arises in the function theory. One such function is *Gaussian Radial Basis Function* (GRBF) given as:

$$g_{\sigma^2}(r) :=_{\text{def}} \exp(-\sigma^2 r^2); \sigma > 0.$$

Let  $\|\cdot\|_2$  be the usual Euclidean norm on  $\mathbf{R}^d$ , this function is comfortably synonymous to its kernel notion which is famously called as the GRBF Kernel given as  $K_{\sigma}(\mathbf{x}, \mathbf{z}) :=_{\text{def}} g_{\sigma^2}(\|\mathbf{x} - \mathbf{z}\|_2)$ . Explicitly that is

$$K_{\sigma}(\mathbf{x}, \mathbf{z}) = \exp(-\sigma^2 \|\mathbf{x} - \mathbf{z}\|_2^2); \sigma > 0.$$

The GRBF Kernel is a building block for various learning architecture such as spatial statistics [Ste99] dynamical system identification [tRKJ19], machine learning [WR06] to name a few. This manuscript extend the idea of GRBF Kernel to what called as the *Generalized GRBF Kernel* (GGRBF Kernel) introduced in [Sin23a].

**Definition 1.1.** Let  $\sigma > 0$  and  $\sigma_0 \geq 0$  then the GGRBF Kernel is defined as:

$$(1) \quad \begin{aligned} K_{\sigma, \sigma_0}(\mathbf{x} - \mathbf{z}) &:=_{def} g_{\sigma^2}(\|\mathbf{x} - \mathbf{z}\|_2) e^{\left(g_{\sigma_0^2}(\|\mathbf{x} - \mathbf{z}\|_2) - 1\right)} \\ &= e^{-\sigma^2 \|\mathbf{x} - \mathbf{z}\|_2^2} e^{-\sigma_0^2 (\|\mathbf{x} - \mathbf{z}\|_2^2) - 1}. \end{aligned}$$

Note that if  $\sigma_0 = 0$ , then we get the traditional GRBF kernel. The GGRBF was introduced in [KKA<sup>+</sup>20] to provide better results in contrast to GRBF results in terms of convergence and stability for interpolation problems on Franke's test function and Runge's function or solving the system with Tikhonov regularization and Riley's algorithm as well.

Taking much of the inspiration from [KKA<sup>+</sup>20], the application of GGRBF Kernel was documented in [Sin23a] in terms of *support vector machine* (SVM), *kernel regression* and pattern recognition via the *activation function for neural network*.

These state-of-the-art methods in learning architecture are leveraged by a peculiar topic from Hilbert function space called as *Reproducing Kernel Hilbert Space* (RKHS) [Aro50]. The analysis from the RKHS theory for the GRBF Kernel has already been established by [SHS06] in which answers related to the norms and feature space were answered. However, with the present empirical evidence supporting better results obtained by employing the GGRBF kernel, it becomes important to perform the same investigation for the GGRBF Kernel.

The present paper is organized as follows: we have essential preliminaries of RKHS in Section 2. Then we have results from the function theory in Section 3 followed by empirical comparison results in Section 4.

## 2. NOTATION & PRELIMINARIES

**2.1. Hypergeometric Function Notation.** We recall important basic calculus results related to the *Generalized Hypergeometric Function*  ${}_pF_q \left[ \begin{matrix} a_1 & a_2 & \dots & a_p \\ b_1 & b_2 & \dots & b_q \end{matrix} ; z \right]$  [Bar06]. With the help of Pochhammer symbol [AS68] (rising factorial notation) given as  $(a)_k = \frac{\Gamma(a+k)}{\Gamma(a)} = a(a+1)\dots(a+k-1)$ , then  ${}_pF_q \left[ \begin{matrix} a_1 & a_2 & \dots & a_p \\ b_1 & b_2 & \dots & b_q \end{matrix} ; z \right]$  is given as

$$(2) \quad {}_pF_q \left[ \begin{matrix} a_1 & a_2 & \dots & a_p \\ b_1 & b_2 & \dots & b_q \end{matrix} ; z \right] :=_{def} \sum_{l=0}^{\infty} \frac{\prod_{i=1}^p (a_i)_l z^l}{\prod_{i=1}^q (b_i)_l l!}.$$

**Example 2.1.** We have the summation  $\sum_{l=0}^{\infty} \frac{1}{(l+x)^{n+1}} \frac{1}{l!}$  in terms of the Generalized Hypergeometric Function given as:

$$\begin{aligned} \sum_{l=0}^{\infty} \frac{1}{(l+x)^{n+1}} \frac{1}{l!} &= \sum_{l=0}^{\infty} \left( \frac{\Gamma(l+x)}{\Gamma(l+x+1)} \right)^{n+1} \frac{1}{l!} \\ &= \sum_{l=0}^{\infty} \left( \frac{(x)_l \Gamma(x)}{(x+1)_l \Gamma(x+1)} \right)^{n+1} \frac{1}{l!} \\ &= \frac{1}{x^{n+1}} {}_{n+1}F_{n+1} \left[ \begin{matrix} x \\ x+1 \end{matrix} ; 1 \right]. \end{aligned}$$

The example presented above will be useful for further great details in the present manuscript. So to avoid heavy-notation-clutter, we write

$$(3) \quad {}_{n+1}F_{n+1} \left[ \begin{matrix} x \\ x+1 \end{matrix} ; 1 \right] :=_{notation} \mathcal{F}_{n,x,1}$$

from now on-wards upon its need. Note that  $\mathcal{F}_{n,\infty,1} = e$ .

**2.2. Field Notation.** The set of natural numbers in union with 0 is denoted by  $\mathbf{W}$ , that is  $\mathbf{W} := 0, 1, 2, \dots$ . We use Kronecker delta  $\delta_{nm}$  on non-negative integers  $n$  and  $m$  to depict that,  $\delta_{nm} = 1$  whenever  $n = m$  and  $\delta_{nm} = 0$  if  $n \neq m$ . We denote a complex number  $z = x + iy$  where  $x$  and  $y \in \mathbf{R}$ . With that  $z$ , its conjugate-part is given as  $\bar{z} = x - iy$  along with its absolute value as  $|z|^2 = z \cdot \bar{z} = x^2 + y^2$ . We reserve symbol  $\mathbf{K}$  to treat with choice of fields on which we will operate upon; in particular  $\mathbf{K}$  can either be  $\mathbf{R}$  or  $\mathbf{C}$ .

**2.3. Tensor Product Notation.** We recall the *tensor product* between two functions, say  $f_1, f_2 : X \rightarrow \mathbf{K}$  given as  $f_1 \otimes f_2 : X \times X \rightarrow \mathbf{K}$ . Then, for all  $x, x' \in X$  the tensor product  $f_1 \otimes f_2$  is defined as  $f_1 \otimes f_2(x, x') := f_1(x)f_2(x')$ .

**2.4. Preliminaries.**

**Definition 2.2.** Let  $X = \emptyset$ , then a function  $k : X \times X \rightarrow \mathbf{K}$  is called the kernel on  $X$  if there exists a  $\mathbf{K}$ -Hilbert space  $(H, \langle \cdot, \cdot \rangle_H)$  accompanied by a map  $\Phi : X \rightarrow H$  such that  $\forall x, x' \in X$ , we have

$$(4) \quad k(x, x') = \langle \Phi(x'), \Phi(x) \rangle_H.$$

We regard  $\Phi$  as the feature map and  $H$  as the feature space of  $k$ .

Now that we have introduced the basic notion from the kernel theory in the definition provided above, we can now comfortably define the building block of this paper: *Reproducing Kernel Hilbert Space, RKHS*.

**Definition 2.3.** Let  $X = \emptyset$  and  $(H, \langle \cdot, \cdot \rangle_H)$  be the Hilbert function space over  $X$ .

- (1) The space  $H$  is called as the **reproducing kernel Hilbert space (RKHS)** if  $\forall x \in X$ , the evaluation functional  $\mathcal{E}_x : H \rightarrow \mathbf{K}$  defined as  $\mathcal{E}_x(f) := f(x)$ ,  $f \in H$  is continuous.

**Definition 2.4.** A function  $k : X \times X \rightarrow \mathbf{K}$  is called **reproducing kernel** of  $H$  if we have:

- (1)  $k(\cdot, x) \in H \forall x \in X$ , that is  $\|k(\cdot, x)\|_H < \infty$ , and  
(2)  $k(\cdot, \cdot)$  has the reproducing property; that is

$$f(x) = \langle f, k(\cdot, x) \rangle_H \quad \forall f \in H \text{ and } x \in X.$$

It is worth-full to mention that the norm convergence yields the point-wise convergence inside RKHS. This fact can be readily learned due to the continuity of evaluation functional. This is demonstrated as follows for an arbitrary  $f \in H$  and  $\{f_n\}_n \in H$  with  $\|f - f_n\|_H \rightarrow 0$  as  $n \rightarrow \infty$ , then

$$\begin{aligned} \lim_{n \uparrow \infty} f_n(x) &= \lim_{n \uparrow \infty} \mathcal{E}_x(f_n) \\ &=_{(\text{continuity of } \mathcal{E}_x)} \mathcal{E}_x(f) \\ &= f(x). \end{aligned}$$

Now, we will state an important theorem from [Aro50] which dictates the relationship between the reproducing kernel of the RKHS  $H$  and the orthonormal basis of it.

**Theorem 2.5** ([Aro50]). *Let  $H$  be an RKHS over an nonempty set  $X$ , Then  $k : X \times X \rightarrow \mathbf{K}$  defined as  $k(x, x') := \langle \mathcal{E}_x, \mathcal{E}_{x'} \rangle_H$  for  $x, x' \in X$  is the only reproducing kernel of  $H$ . Additionally, for some index set  $\mathcal{I}$ , if we have  $\{\mathbf{e}_i\}_{i \in \mathcal{I}}$  as an orthonormal basis (ONB) then for all  $x, x' \in X$ , we have*

$$(5) \quad k(x, x') = \sum_{i \in \mathcal{I}} \mathbf{e}_i(x) \overline{\mathbf{e}_i(x')},$$

with an absolute convergence.

### 3. FUNCTION SPACE

Let  $d \in \mathbf{N}$ ,  $\sigma > 0$  and  $\sigma_0 \geq 0$  and  $f$  be a holomorphic function  $f : \mathbf{C}^d \rightarrow \mathbf{C}$ , we write first the measure of our interest:

$$(6) \quad d\mu_{\sigma, \sigma_0, d}(\mathbf{z}) := e^{-\sigma^2|\mathbf{z}|^2} e^{-\sigma_0|\mathbf{z}|^2 - 1} dV_{\mathbf{C}^d}(\mathbf{z}),$$

Here, ' $dV_{\mathbf{C}^d}(\mathbf{z})$ ' is the usual Lebesgue measure on entire  $\mathbf{C}^d$ . For  $d = 1$ , we write simply  $d\mu_{\sigma, \sigma_0}(z)$  to denote the typical Lebesgue area measure on  $\mathbf{C}$ . We now provide the inner product associated with this measure as:

$$(7) \quad \langle f, g \rangle_{\sigma, \sigma_0, \mathbf{C}^d} := \mathcal{N}_{\sigma, \sigma_0, d} \int_{\mathbf{C}^d} f(\mathbf{z}) \overline{g(\mathbf{z})} d\mu_{\sigma, \sigma_0}(\mathbf{z}).$$

Here, ‘ $\mathcal{N}_{\sigma,\sigma_0,d}$ ’ is the normalization constant whose value is explicitly given as  $(e^{\sigma^2/2\pi})^d$ . Once we have defined the inner product for the space, the norm for holomorphic function  $f : \mathbf{C}^d \rightarrow \mathbf{C}$  is:

$$(8) \quad \|f\|_{\sigma,\sigma_0,\mathbf{C}^d}^2 := \left(\frac{e\sigma^2}{2\pi}\right)^d \int_{\mathbf{C}^d} |f(\mathbf{z})|^2 d\mu_{\sigma,\sigma_0}(\mathbf{z}).$$

We write

$$(9) \quad H_{\sigma,\sigma_0,\mathbf{C}^d} := \{f : \mathbf{C}^d \rightarrow \mathbf{C} \text{ s.t. } \|f\|_{\sigma,\sigma_0,\mathbf{C}^d} < \infty\}.$$

Once we have defined norm in (8) and the associated Hilbert space in (9), we can provide the following formulation which makes the Hilbert space  $H_{\sigma,\sigma_0,\mathbf{C}^d}$  as an RKHS.

**Lemma 3.1.** *For all  $\sigma > 0$ ,  $\sigma_0 \geq 0$  and all compact sets  $K \subset \mathbf{C}^d$ , there exists a positive constant  $c_{\sigma,\sigma_0,d}$  such that for all  $\mathbf{z} \in K$  and  $f \in H_{\sigma,\sigma_0,\mathbf{C}^d}$ , we have*

$$(10) \quad |f(\mathbf{z})| \leq c_{\sigma,\sigma_0,d} \|f\|_{\sigma,\sigma_0,\mathbf{C}^d}.$$

*Proof.* Denote  $\mathbb{B}_{(0,1)}$  as the complex unit ball in  $\mathbf{C}$ . Define

$$c_{\sigma,\sigma_0,d} := \sup_{\mathbf{z} \in K + \mathbb{B}_{(0,1)}^d} \left\{ e^{-\sigma^2|\mathbf{z}|^2} e^{e^{-\sigma_0^2|\mathbf{z}|^2} - 1} \right\}.$$

In the spirit of [SHS06, Lemma-3, Page 4639], we have

$$\prod_{j=1}^d r_j |f(\mathbf{z})|^2 \leq \frac{1}{(2\pi)^d} \prod_{j=1}^d r_j \int_{[0,2\pi]^d} |f(z_1 + r_1 e^{i\theta_1}, \dots, z_d + r_d e^{i\theta_d})|^2 d\theta.$$

Integration of above with respect to  $(r_1, \dots, r_d) \in [0, 1]^d$  yields:

$$\begin{aligned} |f(\mathbf{z})|^2 &\leq \frac{1}{(2\pi)^d} \int_{\mathbf{z} + \mathbb{B}_{(0,1)}^d} |f(\mathbf{z}')|^2 dV(\mathbf{z}') \\ &\leq \frac{c_{\sigma,\sigma_0,d}}{(2\pi)^d} \int_{\mathbf{z} + \mathbb{B}_{(0,1)}^d} |f(\mathbf{z}')|^2 e^{-\sigma^2|\mathbf{z}'|^2} e^{e^{-\sigma_0^2|\mathbf{z}'|^2} - 1} dV(\mathbf{z}') \\ &\leq \frac{c_{\sigma,\sigma_0,d}}{(e\sigma^2)^d} \|f\|_{\sigma,\sigma_0,d}^2. \end{aligned}$$

In particular, we have  $c_{\sigma,\sigma_0,d} = \sqrt{c_{\sigma,\sigma_0,d}/(e\sigma^2)^d}$  and hence the result is established.  $\square$

Establishing Lemma 3.1 yields immediately that  $H_{\sigma,\sigma_0,\mathbf{C}^d}$  is indeed an RKHS and we state here as an important follow-up corollary.

**Corollary 3.2.** *The space  $(H_{\sigma,\sigma_0,\mathbf{C}^d}, \langle \cdot, \cdot \rangle_{\sigma,\sigma_0,\mathbf{C}^d})$  is a RKHS for all  $\sigma > 0$  and  $\sigma_0 \geq 0$ .*

**3.1. Orthonormal Basis.** We will need following technical result to establish the orthonormal basis (ONB) for  $H_{\sigma, \sigma_0, \mathbf{C}^d}$ .

**Lemma 3.3.** *For every  $\sigma > 0, \sigma_0 \geq 0$  and  $n, m \in \mathbf{W}$ , we have*

$$(11) \quad \int_{\mathbf{C}} z^n \overline{z^m} d\mu_{\sigma, \sigma_0}(z) = \left( \sqrt{\frac{2\pi n!}{e\sigma^{2n+2}}} \mathcal{F}_{n, \hat{\sigma}, 1} \sqrt{\frac{2\pi m!}{e\sigma^{2m+2}}} \mathcal{F}_{m, \hat{\sigma}, 1} \right) \delta_{nm}$$

where  $\hat{\sigma} = \sigma_0^2/\sigma^2$  and  $\mathcal{F}_{n, \hat{\sigma}, 1}$  is defined in (3).

*Proof.* Employ the polar coordinate of  $z$  to have:

$$(12) \quad \int_{\mathbf{C}} z^n \overline{z^m} d\mu_{\sigma, \sigma_0}(z) = \int_0^\infty r^{n+m} e^{-\sigma^2 r^2} e^{e^{-\sigma_0^2 r^2} - 1} r dr \int_0^{2\pi} e^{i(n-m)\theta} d\theta.$$

The quantity  $\int_0^\infty r^{n+m} e^{-\sigma^2 r^2} e^{e^{-\sigma_0^2 r^2} - 1} r dr \int_0^{2\pi} e^{i(n-m)\theta} d\theta$  is 0 when  $n \neq m$ . Now, assume that  $n = m$  in (12), then:

$$\begin{aligned} \int_{\mathbf{C}} z^n \overline{z^m} d\mu_{\sigma, \sigma_0}(z) &= 2\pi \int_0^\infty r^{2n} e^{-\sigma^2 r^2} e^{e^{-\sigma_0^2 r^2} - 1} r dr \\ &= \frac{2\pi}{e(\sigma^2)^{n+1}} \int_0^\infty s^n e^{-s} e^{e^{-\sigma_0^2/\sigma^2 s} - 1} ds \\ &= \frac{2\pi \Gamma(n+1)}{e(\sigma^2)^{n+1}} \sum_{l=0}^\infty \frac{1}{l!(l\hat{\sigma} + 1)^{n+1}} \\ &= \frac{2\pi n!}{e\sigma^{2n+2}} \mathcal{F}_{n, \hat{\sigma}, 1} \quad (\text{use (3)}). \end{aligned}$$

Thus the result prevails. □

In the light of Theorem 2.5, we have to determine the ONB of  $H_{\sigma, \sigma_0, \mathbf{C}^d}$ .

**Theorem 3.4.** *Let  $\sigma > 0, \sigma_0 \geq 0$  and  $n \in \mathbf{W}$ . Define  $\{\mathbf{e}_n\}_{n \in \mathbf{W}} : \mathbf{C} \rightarrow \mathbf{C}$  by*

$$(13) \quad \mathbf{e}_n(z) := \sqrt{\frac{\sigma^{2n}}{n! \mathcal{F}_{n, \hat{\sigma}, 1}}} z^n \quad \forall z \in \mathbf{C}.$$

*Then the tensor-product system  $(\mathbf{e}_{n_1} \otimes \cdots \otimes \mathbf{e}_{n_d})_{n_1, \dots, n_d \geq 0}$  forms the ONB of  $H_{\sigma, \sigma_0, \mathbf{C}^d}$ .*

*Proof.* We establish our result for  $d = 1$  for the initial basic understanding. For this, let us show that  $\{\mathbf{e}_n\}_{n \in \mathbf{W}}$  forms an orthonormal system. So, consider  $z \in \mathbf{C}$  and let  $m, n \in \mathbf{W}$ .

Then,

$$\begin{aligned}
\langle \mathbf{e}_n, \mathbf{e}_m \rangle_{\sigma, \sigma_0} &= \frac{e\sigma^2}{2\pi} \int_{\mathbf{C}} \mathbf{e}_n(z) \overline{\mathbf{e}_m(z)} d\mu_{\sigma, \sigma_0}(z) \\
&= \frac{e\sigma^2}{2\pi} \sqrt{\frac{\sigma^{2n}}{n! \mathcal{F}_{n, \hat{\sigma}, 1}}} \sqrt{\frac{\sigma^{2m}}{m! \mathcal{F}_{m, \hat{\sigma}, 1}}} \int_{\mathbf{C}} z^n \overline{z^m} d\mu_{\sigma, \sigma_0}(z) \\
&= \begin{cases} 1 & \text{if } n = m \\ 0 & \text{otherwise} \end{cases} \quad (\text{use Lemma 3.3}).
\end{aligned}$$

The above result concludes that  $\{\mathbf{e}_n\}_{n \in \mathbf{W}}$  is actually an orthonormal system. To this end, we have to establish that it is also complete. So, for this, pick  $f \in H_{\sigma, \sigma_0, \mathbf{C}}$  with  $f(z) = \sum_{l=0}^{\infty} a_l z^l$  and observe that

$$\begin{aligned}
\langle f, \mathbf{e}_n \rangle_{\sigma, \sigma_0} &= \frac{e\sigma^2}{2\pi} \int_{\mathbf{C}} f(z) \overline{\mathbf{e}_n(z)} d\mu_{\sigma, \sigma_0}(z) \\
&= \frac{e\sigma^2}{2\pi} \sum_{l=0}^{\infty} a_l \int_{\mathbf{C}} z^l \overline{\mathbf{e}_n(z)} d\mu_{\sigma, \sigma_0}(z) \\
&= \frac{e\sigma^2}{2\pi} \sqrt{\frac{\sigma^{2n}}{n! \mathcal{F}_{n, \hat{\sigma}, 1}}} \sum_{l=0}^{\infty} a_l \int_{\mathbf{C}} z^l \overline{z^n} d\mu_{\sigma, \sigma_0}(z) \\
&= \frac{e\sigma^2}{2\pi} \sqrt{\frac{\sigma^{2n}}{n! \mathcal{F}_{n, \hat{\sigma}, 1}}} \sum_{l=0}^{\infty} a_l \left( \sqrt{\frac{2\pi l!}{e\sigma^{2l+2}} \mathcal{F}_{n, \hat{\sigma}, 1}} \sqrt{\frac{2\pi n!}{e\sigma^{2n+2}} \mathcal{F}_{n, \hat{\sigma}, 1}} \right) \delta_{ln} \\
&= \sqrt{\frac{\sigma^{2n}}{n! \mathcal{F}_{n, \hat{\sigma}, 1}}} a_n \frac{n! \mathcal{F}_{n, \hat{\sigma}, 1}}{\sigma^{2n}} \\
&= \left[ \sqrt{\frac{\sigma^{2n}}{n! \mathcal{F}_{n, \hat{\sigma}, 1}}} \right]^{-1} a_n.
\end{aligned}$$

Since the constant  $\sigma^{2n}/n! \mathcal{F}_{n, \hat{\sigma}, 1} \neq 0$  for any choice of  $n$ , hence, the condition that  $\langle f, \mathbf{e}_n \rangle = 0$  for all  $n \in \mathbf{W}$  yields that  $a_n = 0$  for all  $n \in \mathbf{W}$ , which results in conclusion that  $f \equiv 0$ . Therefore,  $\{\mathbf{e}_n\}_{n \in \mathbf{W}}$  is complete. Now, we establish these results in  $d$ -dimensional situation by employing the tensor product notation Subsection 2.3. To this end, we see that

$$\langle \mathbf{e}_{n_1} \otimes \cdots \otimes \mathbf{e}_{n_d}, \mathbf{e}_{m_1} \otimes \cdots \otimes \mathbf{e}_{m_d} \rangle_{\sigma, \sigma_0, d} = \prod_{j=1}^d \langle \mathbf{e}_{n_j}, \mathbf{e}_{m_j} \rangle_{\sigma, \sigma_0}.$$

Hence the orthonormality of  $\{\mathbf{e}_{n_1} \otimes \cdots \otimes \mathbf{e}_{n_d}\}_{n_1, \dots, n_d \in \mathbf{W}^d}$  is established due to the orthonormality of each  $\langle \mathbf{e}_{n_j}, \mathbf{e}_{m_j} \rangle_{\sigma, \sigma_0}$ . We still need to ensure that this  $d$ -dimensional orthonormal

system is complete. Now, observe

$$\begin{aligned} \langle f, \mathbf{e}_{n_1} \otimes \cdots \otimes \mathbf{e}_{n_d} \rangle_{\sigma, \sigma_0, d} &= \left( \frac{e\sigma^2}{2\pi} \right)^d \int_{\mathbf{C}^d} f(\mathbf{z}) \overline{\mathbf{e}_{n_1} \otimes \cdots \otimes \mathbf{e}_{n_d}(\mathbf{z})} d\mu_{\sigma, \sigma_0, \mathbf{C}^d}(\mathbf{z}) \\ &= \left( \frac{e\sigma^2}{2\pi} \right)^d \sum_{l_1, \dots, l_d}^{\infty} a_{l_1, \dots, l_d} \mathbb{I}_{l, d}, \end{aligned}$$

where  $\mathbb{I}_{l, d} = \int_{\mathbf{C}^d} \mathbf{z}^l (\mathbf{e}_{n_1} \otimes \cdots \otimes \mathbf{e}_{n_d}(\bar{\mathbf{z}})) d\mu_{\sigma, \sigma_0, \mathbf{C}^d}(\mathbf{z})$ . We further can simplify  $\mathbb{I}_d$  as follows:

$$\begin{aligned} \mathbb{I}_{l, d} &= \int_{\mathbf{C}^d} \mathbf{z}^l \mathbf{e}_{n_1}(\bar{z}_1) \wedge \cdots \wedge \mathbf{e}_{n_d}(\bar{z}_d) d\mu_{\sigma, \sigma_0}(z_1) \wedge \cdots \wedge d\mu_{\sigma, \sigma_0}(z_d) \\ &= \prod_{j=1}^d \left( \int_{\mathbf{C}} z_j^{l_j} \mathbf{e}_{n_j}(\bar{z}_j) d\mu_{\sigma, \sigma_0}(z_j) \right) \\ &= \prod_{j=1}^d \left( \int_{\mathbf{C}} z_j^{l_j} \bar{z}_j^{n_j} d\mu_{\sigma, \sigma_0}(z_j) \right) \\ &= \prod_{j=1}^d \left( \sqrt{\frac{2\pi l_j!}{e\sigma^{2l_j+2}} \mathcal{F}_{l_j, \hat{\sigma}, 1}} \sqrt{\frac{2\pi n_j!}{e\sigma^{2n_j+2}} \mathcal{F}_{n_j, \hat{\sigma}, 1}} \right) \delta_{l_j, n_j} a_{l_1, \dots, l_d}. \end{aligned}$$

Finally,

$$\left( \frac{e\sigma^2}{2\pi} \right)^d \sum_{l_1, \dots, l_d}^{\infty} a_{l_1, \dots, l_d} \mathbb{I}_{l, d} = \left( \prod_{j=1}^d \left[ \sqrt{\frac{\sigma^{2n_j}}{n_j! \mathcal{F}_{n_j, \hat{\sigma}, 1}}} \right]^{-1} \right) a_{n_1, \dots, n_d}.$$

The further result for completeness in  $d$ -dimension follows a routine procedure from single-dimension case as already discussed before.  $\square$

The following theorem provides the reproducing kernel for the Hilbert space  $H_{\sigma, \sigma_0, \mathbf{C}^d}$  defined in (9).

**Theorem 3.5.** *For  $\sigma > 0$ ,  $\sigma_0 \geq 0$  and  $\hat{\sigma} = \sigma^2/\sigma_0^2$ , the reproducing kernel for the space  $H_{\sigma, \sigma_0, \mathbf{C}^d}$  is given as*

$$(14) \quad K(\mathbf{z}, \mathbf{w}) := \sum_{n_1, \dots, n_d=0}^{\infty} \lambda_n (\mathbf{z}\bar{\mathbf{w}})^n,$$

where multi-index notation is employed:  $n = (n_1, \dots, n_d)$  and  $\lambda_n = \prod_{i=1}^d \frac{\sigma^{2n_i}}{n_i! \mathcal{F}_{n_i, \hat{\sigma}, 1}}$ .

*Proof.* We will demonstrate the desired proof as follows:



(1) For  $\mathbf{w} \in \mathbf{C}^d$ , we will show that  $\|K(\cdot, \mathbf{w})\|_{\sigma, \sigma_0, d} < \infty$ .

$$\begin{aligned}
\|K(\cdot, \mathbf{w})\|_{\sigma, \sigma_0, d}^2 &= \left(\frac{e\sigma^2}{2\pi}\right)^d \int_{\mathbf{C}^d} |K(\mathbf{z}, \mathbf{w})|^2 d\mu_{\sigma, \sigma_0, d}(\mathbf{z}) \\
(15) \quad &= \left(\frac{e\sigma^2}{2\pi}\right)^d \sum_{n_1, \dots, n_d}^{\infty} \sum_{m_1, \dots, m_d}^{\infty} \lambda_n \lambda_m \mathbf{w}^n \overline{\mathbf{w}}^m \int_{\mathbf{C}^d} \mathbf{z}^n \overline{\mathbf{z}}^m d\mu_{\sigma, \sigma_0, d}(\mathbf{z}) \\
(16) \quad &= \left(\frac{e\sigma^2}{2\pi}\right)^d \sum_{n_1, \dots, n_d}^{\infty} \lambda_n^2 |\mathbf{w}|^{2n} \left( \prod_{n_i=1}^d \int_{\mathbf{C}} z_i^{n_i} \overline{z}_i^{m_i} d\mu_{\sigma, \sigma_0}(z_i) \right) \\
&= \left(\frac{e\sigma^2}{2\pi}\right)^d \sum_{n_1, \dots, n_d}^{\infty} \lambda_n^2 |\mathbf{w}|^{2n} \left( \prod_{n_i=1}^d \frac{2\pi n_i!}{\sigma^{2n_i+2}} \mathcal{F}_{n_i, \hat{\sigma}, 1} \right) \\
&= \sum_{n_1, \dots, n_d}^{\infty} \frac{|\mathbf{w}|^{2n}}{\prod_{i=1}^d \frac{n_i!}{\sigma^{2n_i}} \mathcal{F}_{n_i, \hat{\sigma}, 1}}.
\end{aligned}$$

We used the result of Theorem 3.4 from (15) to(16). For all  $\mathbf{w} \in \mathbf{C}^d$ , the quantity  $\sum_{n_1, \dots, n_d}^{\infty} \frac{|\mathbf{w}|^{2n}}{\prod_{i=1}^d (n_i!/\sigma^{2n_i}) \mathcal{F}_{n_i, \hat{\sigma}, 1}}$  achieves convergence. This implies that  $\|K(\cdot, \mathbf{w})\|_{\sigma, \sigma_0, d} < \infty$  for all  $\mathbf{w} \in \mathbf{C}^d$ . Therefore, the kernel function  $K(\cdot, \mathbf{w}) \in H_{\sigma, \sigma_0, \mathbf{C}^d}$ .

(2) Now, in order to establish the reproducing property of  $K(\cdot, \mathbf{w})$  pick an arbitrary  $f = \sum_{n_1, \dots, n_d}^{\infty} a_{n_1, \dots, n_d} \mathbf{w}^n \in H_{\sigma, \sigma_0, \mathbf{C}^d}$ . Then, consider the inner product of  $f$  with  $K(\cdot, \mathbf{w})$  as follows:

$$\begin{aligned}
\langle f, K(\cdot, \mathbf{w}) \rangle_{\sigma, \sigma_0, \mathbf{C}^d} &= \left(\frac{e\sigma^2}{2\pi}\right)^d \int_{\mathbf{C}^d} f(\mathbf{z}) \overline{K(\mathbf{z}, \mathbf{w})} d\mu_{\sigma, \sigma_0, \mathbf{C}^d}(\mathbf{z}) \\
&= \left(\frac{e\sigma^2}{2\pi}\right)^d \sum_{n_1, \dots, n_d}^{\infty} \sum_{l_1, \dots, l_d}^{\infty} a_{n_1, \dots, n_d} \lambda_{l_1, \dots, l_d} \mathbf{w}^n \left( \prod_{i=1}^d \frac{2\pi}{e\sigma^2} \frac{\sigma^{2n_i}}{n_i! \mathcal{F}_{n_i, \hat{\sigma}, 1}} \right) \\
&= \sum_{n_1, \dots, n_d=0}^{\infty} a_{n_1, \dots, n_d} \mathbf{w}^n \\
&= f(\mathbf{w}).
\end{aligned}$$

Hence, the desired result is achieved. □

The proof in the preceding theorem to demonstrate reproducing kernel nature of  $K(\mathbf{z}, \mathbf{w})$  of  $H_{\sigma, \sigma_0, \mathbf{C}^d}$  utilizes the basic machinery borrowed from the two-part definition for reproducing kernel given in Definition 2.4.

## 4. EMPIRICAL EVIDENCE AND RESULTS COMPARISON

## 4.1. Kernel Regression.

4.1.1. *Example-1.* Kernel regression of  $f(x) = e^{\frac{(1-9x^2)}{4}} + \tan x + x^{\frac{1}{6}} + \sin x^{\vartheta(n)}$  is performed via both GRBF and (1). Here  $\vartheta(n)$  is uniform random distributed number in  $(0, 1)$ ,  $x = n \in \mathbf{Z}_{101}$ .

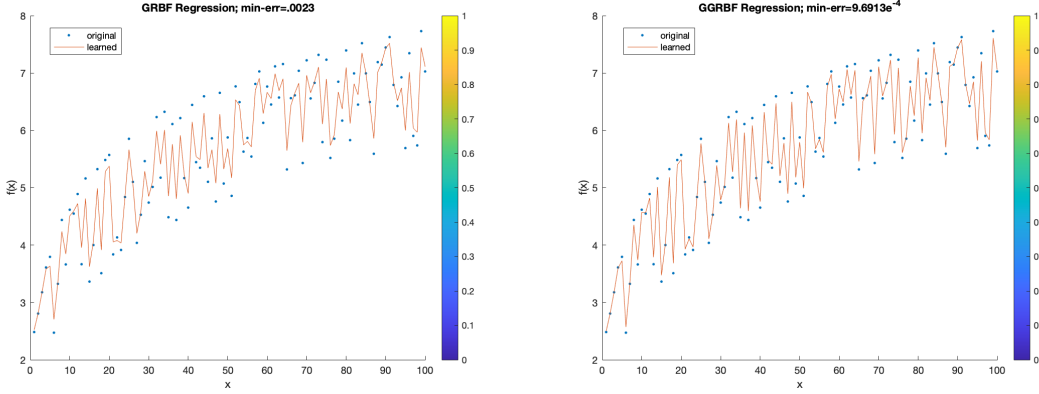


FIGURE 1. [MATLAB] Kernel regression of  $f(x) = e^{\frac{(1-9x^2)}{4}} + \tan x + x^{\frac{1}{6}} + \sin x^{\vartheta(n)}$ .

4.1.2. *Example-2.* Kernel regression of  $f(x) = e^{\sin x - \sin x^2} + \sqrt{2\pi}|x + \cos \vartheta(n)|$  is performed via both GRBF and (1). Here  $\vartheta(n)$  is uniform random distributed number in  $(0, 1)$ ,  $x = n \in \mathbf{Z}_{101}$ .

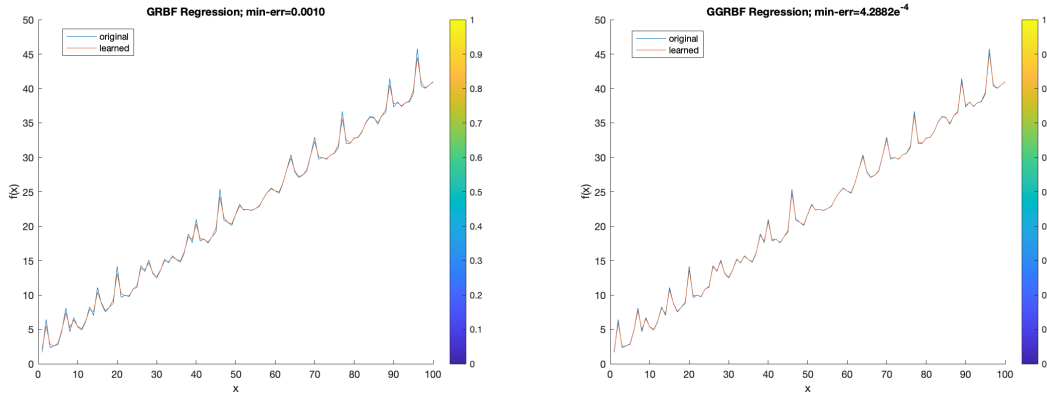


FIGURE 2. [MATLAB] Kernel regression of  $f(x) = e^{\sin x - \sin x^2} + \sqrt{2\pi}|x + \cos \vartheta(n)|$ .

4.2. **Support Vector Machine.** Support vector machine (SVM) is implemented for the the data classification and is performed via different choices of kernels; these kernels includes the traditional *Sigmoid*, GRBF and (1).

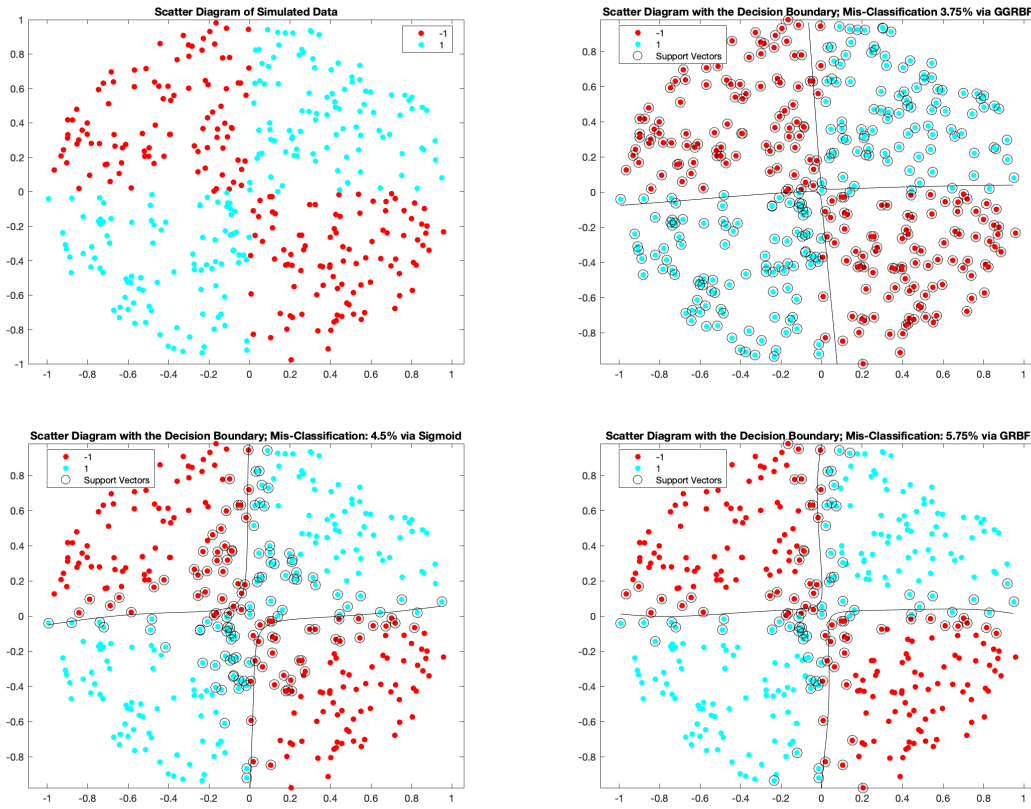


FIGURE 3. [MATLAB] SVM classifier via different kernels.

Out of three kernels, (1) yields the lowest miss-classification for the data of 100 sampled points.

4.3. **Neural Network.** Following examples provide optimally-best results by the (1) employment both as in the usage of *Activation Function* and neural net layer in *deep convolutional neural nets* (DCNN).

4.3.1. *Activation Function.* Consider an  $\alpha$ ReLU activation function, a simple modification of powerful-traditional ReLU activation function from NN, defined as

$$(\alpha\text{ReLU}) \quad f(x) := \begin{cases} x & \text{if } x > 0 \\ \alpha x & \text{if } x \leq 0. \end{cases}$$

In the present experiment, a two 7-layered NNs are constructed; one with the activation function defined by ( $\alpha$ ReLU) and one with (1). Thereafter, following performance tables yields the respective results and comparison for the NNs.

Test Summary:					
13 Passed, 0 Failed, 0 Incomplete, 9 Skipped.					
Time elapsed: 0.17897 seconds.					
Training on single CPU.					
Initializing input data normalization.					
Epoch	Iteration	Time Elapsed (hh:mm:ss)	Mini-batch Accuracy	Mini-batch Loss	Base Learning Rate
1	1	00:00:00	8.59%	2.5717	0.0010
2	50	00:00:04	62.50%	1.3417	0.0010
3	100	00:00:07	88.20%	0.5930	0.0010
4	150	00:00:11	92.97%	0.3817	0.0010
6	200	00:00:14	96.88%	0.2571	0.0010
7	250	00:00:18	99.22%	0.2139	0.0010
8	300	00:00:21	100.00%	0.1152	0.0010
9	350	00:00:25	100.00%	0.0861	0.0010
10	390	00:00:28	100.00%	0.0800	0.0010

accuracy = 0.9774

Test Summary:					
13 Passed, 0 Failed, 0 Incomplete, 9 Skipped.					
Time elapsed: 0.38326 seconds.					
Training on single CPU.					
Initializing input data normalization.					
Epoch	Iteration	Time Elapsed (hh:mm:ss)	Mini-batch Accuracy	Mini-batch Loss	Base Learning Rate
1	1	00:00:00	4.69%	2.9964	0.0010
2	50	00:00:04	70.31%	0.8579	0.0010
3	100	00:00:09	89.06%	0.3620	0.0010
4	150	00:00:13	87.50%	0.3291	0.0010
6	200	00:00:18	96.88%	0.1590	0.0010
7	250	00:00:22	98.44%	0.1274	0.0010
8	300	00:00:27	99.22%	0.0688	0.0010
9	350	00:00:31	100.00%	0.0432	0.0010
10	390	00:00:35	100.00%	0.0350	0.0010

accuracy = 0.9476

FIGURE 4. [MATLAB] Performance comparison (1) ( $L$ ) & ( $\alpha$ ReLU) ( $R$ ) as the NN activation function.

MATLAB script for the activation function of GGRBF is provided in Section 7.

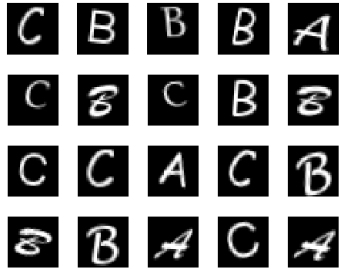
4.3.2. *DCNN.* Above experiments demonstrate the concrete functionality of (1) as an activation function, it further motivates to perform DCNN. Therefore, in pursue of this, a typical DCNN of 7-layered is constructed; one with the activation function defined by ( $\alpha$ ReLU) and one with (1). In the following experiment, the training data contains 1500- $28 \times 28$  gray-scale letter images of  $A$ ,  $B$ , and  $C$  in a 4-D array.



Training on single CPU.					
Initializing input data normalization.					
Epoch	Iteration	Time Elapsed (hh:mm:ss)	Mini-batch Accuracy	Mini-batch Loss	Base Learning Rate
1	1	00:00:00	56.72%	1.1800	0.0100
5	50	00:00:09	98.44%	0.2448	0.0100
10	100	00:00:13	100.00%	0.0043	0.0100
14	150	00:00:16	100.00%	0.0019	0.0100
19	200	00:00:23	100.00%	0.0028	0.0100
23	250	00:00:27	100.00%	0.0012	0.0100
28	300	00:00:32	100.00%	0.0013	0.0100
30	350	00:00:35	100.00%	0.0009	0.0100

accuracy = 0.9633

FIGURE 5. [MATLAB] 96.33% accuracy registered with (1) as DCNN neural layer.



```

Training on single CPU.
Initializing input data normalization.
=====
| Epoch | Iteration | Time Elapsed | Mini-batch | Mini-batch | Base Learning |
|       |          | (M:seconds)  | Accuracy   | Loss        | Rate          |
=====
| 1 | 1 | 00:00:00 | 37.50% | 1.0878 | 0.0100 |
| 5 | 50 | 00:00:03 | 100.00% | 0.0588 | 0.0100 |
| 10 | 100 | 00:00:03 | 100.00% | 0.0145 | 0.0100 |
| 14 | 150 | 00:00:05 | 100.00% | 0.0077 | 0.0100 |
| 19 | 200 | 00:00:06 | 100.00% | 0.0067 | 0.0100 |
| 23 | 250 | 00:00:08 | 100.00% | 0.0043 | 0.0100 |
| 28 | 300 | 00:00:09 | 100.00% | 0.0039 | 0.0100 |
| 30 | 330 | 00:00:10 | 100.00% | 0.0030 | 0.0100 |
=====
accuracy =
0.9187
    
```

FIGURE 6. [MATLAB] 91.87% accuracy registered with ( $\alpha$ ReLU) as DCNN neural layer.

### 5. FUTURE DIRECTIONS

5.1. **Eigen-function expansion of GGRBF.** We recall the *Mercer's Theorem* from [WR06, Theorem 4.2, Page 96].

**Theorem 5.1** (Mercer's Theorem). *Let  $(\mathcal{X}, \mu)$  be a finite measure space and  $k \in L_\infty(\mathcal{X}^2, \mu^2)$  be a kernel such that  $T_k : L_2(\mathcal{X}, \mu) \rightarrow L_2(\mathcal{X}, \mu)$  is positive definite. Let  $\{\phi_i\}_i \in L_2(\mathcal{X}, \mu)$  be the normalized eigenfunctions of  $T_k$  associated with the eigenvalues  $\{\Lambda_i\}_i$ . Then:*

- (1) *the eigenvalues  $\{\Lambda_i\}_i$  are absolutely summable*
- (2)

$$(17) \quad k(\mathbf{x}, \mathbf{x}') = \sum_{i=0}^{\infty} \Lambda_i \phi_i(\mathbf{x}) \phi_i(\mathbf{x}')^*$$

*holds  $\mu^2$  almost everywhere, where the series converges absolutely and uniformly  $\mu^2$  almost everywhere.*

**Example 5.2.** *With the application of Theorem 5.1, we can provide the eigen-function decomposition of  $K_\sigma(x, z) = e^{-\sigma^2(x-z)^2}$  for  $x, z \in \mathbf{R}$ , that is:*

$$(18) \quad e^{-\sigma^2(x-z)^2} = \sum_{i=0}^{\infty} \Lambda_i \phi_i(x) \phi_i(z), \quad \text{where}$$

$$(19) \quad \Lambda_i = \frac{\alpha \sigma^{2i}}{\left(\frac{\alpha^2}{2} \left(1 + \sqrt{1 + \left(\frac{2\sigma}{\alpha}\right)^2}\right) + \frac{\sigma^2}{2}\right)^{i+1/2}}$$

$$(20) \quad \phi_i(x) = \frac{\sqrt[8]{1 + \left(1 + \frac{2\sigma}{\alpha}\right)^2}}{\sqrt{2^i i!}} e^{-\left(\sqrt{1 + \left(\frac{2\sigma}{\alpha}\right)^2} - 1\right) \frac{\alpha^2 x^2}{2}} H_i \left( \sqrt[4]{1 + \left(\frac{2\sigma}{\alpha}\right)^2} \alpha x \right).$$

The expression  $\{H_i(\bullet)\}_i$  in (20) are the Hermite polynomials which are  $L_2$ -orthonormal against the weight  $\alpha/\pi e^{-\alpha^2 x^2}$ ; that is:

$$(21) \quad \int_{\mathbf{R}} \phi_n(x)\phi_m(x)\frac{\alpha}{\pi}e^{-\alpha^2 x^2} dx = \delta_{nm}.$$

We have the graphical representation of first seven Hermite polynomials in following figures Figure 7:

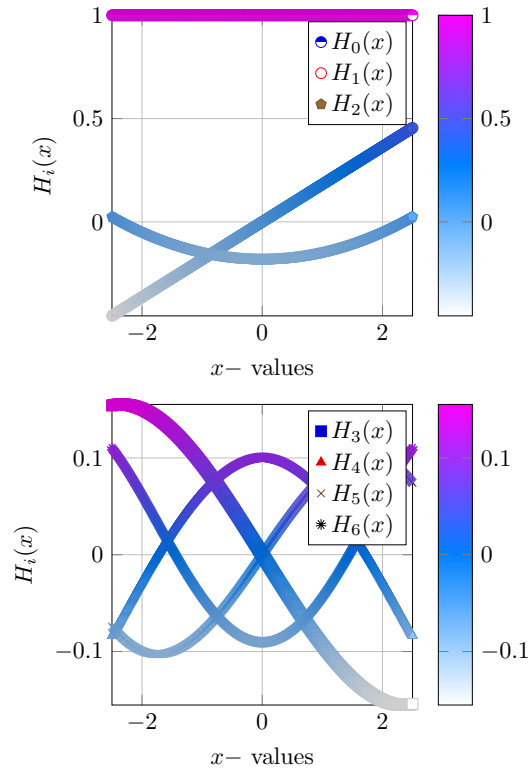


FIGURE 7. First seven Hermite polynomials

Based on the Hermite polynomials [Her64] and as its application for the eigen decomposition analysis for GRBF kernel, we have the following promising future research direction.

In the spirit of the application of the Mercer's Theorem, we know the eigen-function decomposition of the GRBF Kernel. However, presently, we are not fortunate to have such a decomposition for the GGRBF Kernel. A preliminary investigation towards the desired

eigen-function decomposition of GGRBF Kernel (followed from [Ras06, Zhu97, Fas12]) directs us to incorporate a new variety of function defined in (22).

$$(22) \quad \mathcal{H}_n(x) := (-1)^n e^{ax^2} e^{-e^{-bx^2} + 1} \frac{d^n}{dx^n} \left( e^{-ax^2} e^{e^{-bx^2} - 1} \right)$$

into our desired eigen-function decomposition analysis. Here  $a > 0$  and  $b \geq 0$  and therefore, if  $a = 1$  &  $b = 0$  then  $\mathcal{H}_i = H_i$ . The first two expression for  $\mathcal{H}_n(x)$  are explicitly given as:

$$(D1) \quad \mathcal{H}_1(x) = 2ax + 2bx e^{-bx^2},$$

$$(D2) \quad \mathcal{H}_2(x) = -2a + 4b^2 x^2 e^{-bx^2} - 2be^{-bx^2} + \left( 2ax + 2bx e^{-bx^2} \right)^2.$$

The constants  $a$  and  $b$  present in (22) corresponds to the respective constants present in (1); in particular  $a = \sigma^2$  and  $b = \sigma_0^2$ . Following are the graphical presentation of first seven function from the family defined in (22).

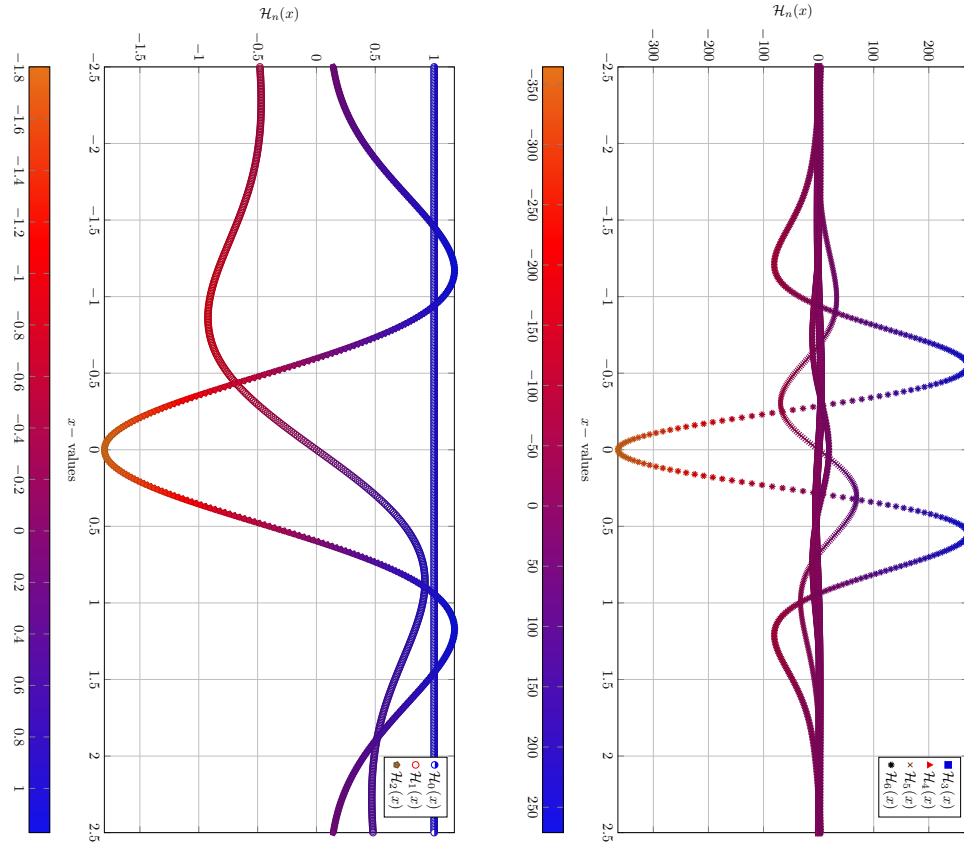


FIGURE 8. Graph of  $\mathcal{H}_n(x)$  for  $n = 0, 1, 2, 3, 4, 5$  and  $6$  with  $a = .091$  &  $b = 0.81$ .

Following TABLE 1 is the compilation of the results documented for the various experiments we discussed so far.

TABLE 1. Compilation of results

AI LEARNING ARCHITECTURE	MATHEMATICAL FUNCTION	FIGURE REF.	MINIMUM ERROR	MISCLASS. %	ACCURACY %
Kernel Regression	GRBF	Figure 1	0.0023	-	-
Kernel Regression	<b>GGRBF</b>	Figure 1	<b><math>9.6913 \times 10^{-4}</math></b>	-	-
Kernel Regression	GRBF	Figure 2	0.0010	-	-
Kernel Regression	<b>GGRBF</b>	Figure 2	<b><math>4.2882 \times 10^{-4}</math></b>	-	-
Support Vector Machine	GRBF	Figure 3	-	5.75	94.25
Support Vector Machine	Sigmoid	Figure 3	-	4.5	95.5
Support Vector Machine	<b>GGRBF</b>	Figure 3	-	<b>3.75</b>	<b>96.25</b>
Activation Function Neural Network	$\alpha$ ReLU	Figure 4	-	5.24	94.76
Activation Function Neural Network	<b>GGRBF</b>	Figure 4	-	<b>2.26</b>	<b>97.74</b>
Deep Convolutional Neural Network	<b>GGRBF</b>	Figure 5	-	<b>3.67</b>	<b>96.33</b>
Deep Convolutional Neural Network	$\alpha$ ReLU	Figure 6	-	8.13	91.87

**Future Direction 5.3.** *Having stated that, we are still in the void knowledge for eigenvalues of the GGRBF Kernel. Additionally, we still need to investigate whether the function introduced in (22) are orthonormal in the sense as the traditional Hermite polynomials are. Therefore, it will be interesting to understand the analysis of the function given in (22).*

**5.2. Operator Theory Analysis for Data-Driven Problems.** Modern data driven problems arising in the field of dynamical systems are captured by the Liouville Operators [tKGJ22], Liouville Weighted Composition Operators [Sin23b, Chapter 2] or Koopman Operators [WKR15] acting over the underlying Hilbert spaces. The work-horse algorithm in the direction of *reduced order modelling* (ROM) techniques is *Dynamic Mode Decomposition* (DMD) [Sch10] which aims to determine the spatio-temporal coherent structures of high-dimensional time-series data is executed by extracting the eigen-observables of the aforementioned operators over the underlying RKHS.

These RKHS are *Bergman-Seigal-Fock Space* [Zhu12] which is generated by the *exponential dot product kernel*. The  $L^2$ -measure for this RKHS is (normalized) Gaussian measure  $(\sigma^2/\pi)^d e^{-\sigma^2|z|^2} dV_{\mathbb{C}^d}(z)$ . Following are the results from the DMD experiment for the vorticity of the fluid flow across the cylinder when the chosen kernel was the GRBF Kernel.



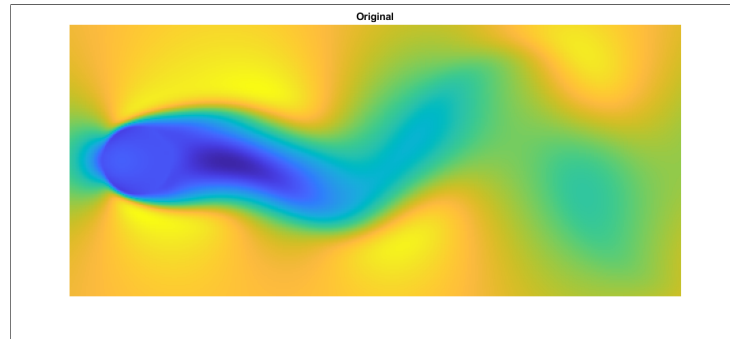


FIGURE 9. Original DMD Experiment for the fluid flow across the cylinder.

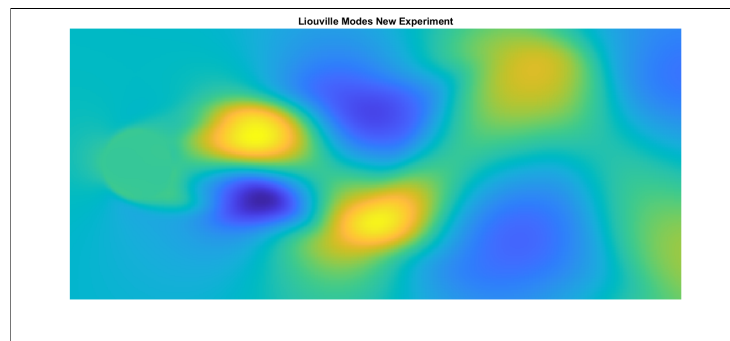


FIGURE 10. 199<sup>th</sup>-Liouville Mode (no noise) via the GGRBF Kernel for the fluid flow across the cylinder.

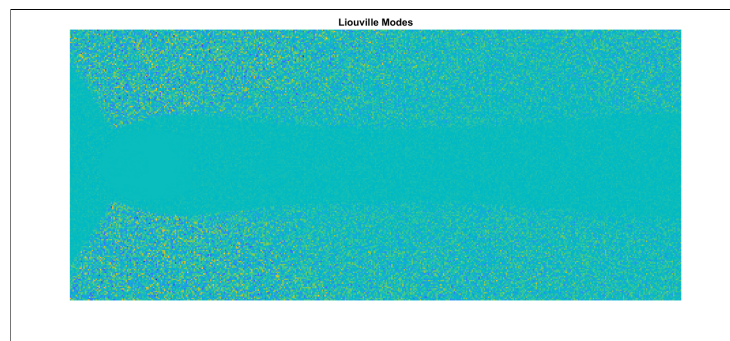


FIGURE 11. 199<sup>th</sup>-Liouville Mode (noise) via the GRBF Kernel for the fluid flow across the cylinder.

Clearly, DMD results by GGRBF in Figure 10 contains visibly-no-noise as compared to results obtain by GRBF in Figure 11.

**Future Direction 5.4.** *We understand the action of Koopman Operators (or composition operators) over the Bergman-Seigal-Fock Space due to the investigation performed by Carswell, MacCluer and Schuster in [CMS03]. On the other hand, [Sin23b, Theorem 2.25, Chapter 2] demonstrates the provable convergence phenomena for dynamical systems by the Liouville weighted composition operators over the Bergman-Seigal-Fock Space. It will be interesting to carry-out the similar operator theoretic investigation over the RKHS introduced in (9).*

## 6. ACKNOWLEDGEMENT

The author would like to thanks reviewer for their precious time on reviewing the present manuscript. In addition to this, author also acknowledges the support of following as well.

- (1) The author acknowledges the support of *Ms. Drishty Singh, 4th Year MSc, Department of Mathematics, Babasaheb Bhimrao Ambedkar University, Lucknow, Uttar Pradesh, India.* She provided the explicit expression of first two functions in (D1) and (D2) from (22). Further analysis of the function in (22) was extended due to these important results.
- (2) The author is thankful for the valuable discussion with Dr. Romit Maulik, *Assistant Professor, Information Sciences and Technology, Institute of Computational and Data Sciences, Pennsylvania State University.* The results in Section 4 were discovered during the research discussion with him in Fall 2022's ending for preparing the research proposal for *Eric and Wendy Schmidt AI in Science Postdoctoral Fellow Program-2023.*
- (3) The empirical results in Section 4 were discovered during the last year of PhD at University of South Florida, where he was supported by DR. JOEL A. ROSENFELD's (PhD advisor) NSF and AFOSR grants (AFOSR Young Investigator Research Program (YIP) Award FA9550-21-1-0134, FA9550-20-1-0127 & ECCS-2027976). The author would like to thanks his advisor's support on this. The RKHS theory present in the first half of this paper was developed while he was at The University of Texas at Tyler.

## 7. MATLAB SCRIPT

**7.1. Neural Net Layer of GGRBF.** In order to execute experiments which employs the neural net layer of activation function as GGRBF, we have to construct it from the scratch. In that regards, following is the MATLAB script for the construction of custom neural net layer for the GGRBF.

```

1 classdef ggrbf < nnet.layer.Layer
2     % Custom GGRBF layer.
3
4     properties (Learnable)

```

```

5      % Layer learnable parameters.
6      % Scaling coefficients.
7      Alpha
8      Beta
9  end
10
11  methods
12      function layer = ggrbf(numChannels, name)
13
14
15          % Set layer name.
16          layer.Name = name;
17
18
19          % Initialize scaling coefficient.
20          layer.Alpha = rand([1 1 numChannels]);
21          layer.Beta = rand([1 1 numChannels]);
22  end
23
24      function Z = predict(layer, X)
25          % Z = predict(layer, X) forwards the input data X
26          % through the layer and outputs the result Z.
27          Z = exp(-(layer.Alpha).^(-2).*X.*X) .* exp(exp(-(layer.
28              Beta).^(-2).*X.*X)-1);
29  end
end

```

## REFERENCES

- [Aro50] Nachman Aronszajn. Theory of reproducing kernels. *Transactions of the American Mathematical Society*, 68(3):337–404, 1950. 2, 4
- [AS68] Milton Abramowitz and Irene A Stegun. *Handbook of mathematical functions with formulas, graphs, and mathematical tables*, volume 55. US Government printing office, 1968. 2
- [Bar06] Ernest William Barnes. V. The asymptotic expansion of integral functions defined by Taylor’s series. *Philosophical Transactions of the Royal Society of London. Series A, Containing Papers of a Mathematical or Physical Character*, 206(402-412):249–297, 1906. 2
- [CMS03] Brent Carswell, Barbara D MacCluer, and Alex Schuster. Composition operators on the Fock Space. *Acta Sci. Math.(Szeged)*, 69(3-4):871–887, 2003. 18
- [Fas12] Fasshauer, Gregory E and McCourt, Michael J. Stable evaluation of Gaussian radial basis function interpolants. *SIAM Journal on Scientific Computing*, 34(2):A737–A762, 2012. 15

- [Her64] M Hermite. *Sur un nouveau développement en série des fonctions*. Imprimerie de Gauthier-Villars, 1864. 14
- [KKA<sup>+</sup>20] N Karimi, S Kazem, D Ahmadian, H Adibi, and LV Ballestra. On a generalized Gaussian radial basis function: Analysis and applications. *Engineering Analysis with Boundary Elements*, 112:46–57, 2020. 2
- [Ras06] Rasmussen, Carl Edward and Williams, Christopher KI and others. *Gaussian Processes for Machine Learning*, volume 1. Springer, 2006. 15
- [Sch10] Peter J Schmid. Dynamic mode decomposition of numerical and experimental data. *Journal of Fluid Mechanics*, 656:5–28, 2010. 16
- [SHS06] Ingo Steinwart, Don Hush, and Clint Scovel. An explicit description of the reproducing kernel Hilbert spaces of Gaussian RBF kernels. *IEEE Transactions on Information Theory*, 52(10):4635–4643, 2006. 2, 5
- [Sin23a] Himanshu Singh. A new kernel function for better AI methods. In *2023 AMS Spring Eastern Sectional Meeting*, number 68-Computer Science, 68T-Artificial Intelligence and 68T07-Artificial Neural Networks and Deep Learning in April 1, 2023. AMS, 2023. 1, 2
- [Sin23b] Himanshu Singh. *Applied Analysis for Learning Architectures*. PhD thesis, University of South Florida, 2023. 16, 18
- [Ste99] Michael L Stein. *Interpolation of spatial data: some theory for kriging*. Springer Science & Business Media, 1999. 1
- [tKGJ22] Joel A ROSENFELD, Rushikesh Kamalapurkar, L Forest Gruss, and Taylor T Johnson. Dynamic mode decomposition for continuous time systems with the Liouville operator. *Journal of Nonlinear Science*, 32:1–30, 2022. 16
- [tRKJ19] Joel A ROSENFELD, Benjamin Russo, Rushikesh Kamalapurkar, and Taylor T Johnson. The occupation kernel method for nonlinear system identification. *arXiv preprint arXiv:1909.11792*, 2019. 1
- [WKR15] Matthew O Williams, Ioannis G Kevrekidis, and Clarence W Rowley. A data-driven approximation of the Koopman operator: Extending dynamic mode decomposition. *Journal of Nonlinear Science*, 25:1307–1346, 2015. 16
- [WR06] Christopher KI Williams and Carl Edward Rasmussen. *Gaussian processes for machine learning*, volume 2. MIT press Cambridge, MA, 2006. 1, 13
- [Zhu97] Zhu, Huaiyu and Williams, Christopher KI and Rohwer, Richard and Morciniec, Michal. Gaussian regression and optimal finite dimensional linear models. *Neural Networks and Machine Learning, 1998, Springer-Verlag*, 1997. 15
- [Zhu12] Kehe Zhu. *Analysis on Fock spaces*, volume 263. Springer Science & Business Media, 2012. 16
- Email address: hsingh@uttyler.edu*

(Visiting Assistant Professor for Academic Year Aug 2023-May 2024) DEPARTMENT OF MATHEMATICS,  
THE UNIVERSITY OF TEXAS AT TYLER, TX 75799, USA